International Journal of Nanoelectronics and Materials
IJNeaM
ISSN 1985-5761 | E-ISSN 2232-1535

Study of Mechanical and Optical Properties of Nano-hydroxyapatite Dispersed PS/PC Blend Nanocomposites

Hadeel Abed 1[a] *, Nahida Hameed 2[b], and Evan Salim 3[c]

[a] *Applied Science Department, University of Technology- Iraq, Baghdad 10001, Iraq*
[b] *Applied Science Department, University of Technology- Iraq, Baghdad 10001, Iraq*
[c] *Applied Science Department, University of Technology- Iraq, Baghdad 10001, Iraq*
** Corresponding author. Tel.: +964 7715752087; e-mail: evan.t.salim@uotechnology.edu.iq*

Received 8 March 2023, Revised 1 May 2023, Accepted 22 May 2023

ABSTRACT

The present investigation deals with the mechanical, structural, and optical properties of chemically fabricated nHAP (Nano hydroxyapatite) nanoparticles filled PC/PS blend nanocomposites. A sequence of PS/PC (100/0, 10%PC/PS, 0/100 wt%/wt %) and nHAP (0.8, 1.6, 3.2, 6.4, and 10 wt %) blend nanocomposites was prepared via solution casting technique. The prepared blend nanocomposites were exposed to XRD, SEM, and FTIR for structural analysis. The optical constants were analyzed utilizing UV-Vis spectroscopy. The XRD, SEM, and FTIR spectrum verified the formation of PC/PS-nHAP blend nanocomposites. The outcomes manifested that the optical constants change with the increase of nHPA concentrations. The mechanical properties were enhanced by the addition of nHAP up to (1.6). The enhancement in mechanical properties suggests that 10%PS/PC blends can be used for packaging material.

Keywords: *Blend nanocomposites, SEM, FTIR, UV-Vis spectroscopy, Band-gap*

1. INTRODUCTION

Composite membranes, as flexible materials, have found various industrial and biomedical applications simultaneously; recent studies have shown an essential improvement in membrane properties by the inclusion of nanoparticles as fillers with a high portion ratio in inorganic polymers [1]. The combination of two parts (polymer and filler) is a result of collecting the advantages of two component systems' parts together [2], for example, flexibility, chemical stability, and elasticity, in addition to the mechanical and thermal stabilities [3]. Polymers, owing to their multipurpose and broad diversity of uses, have been making a global request. The usual polymers utilized in numerous uses as raw materials are polycarbonates, polystyrene, polypropylene, polyethylene, acrylonitrile, and acrylics [1-3].

Among such polymers, polycarbonate (PC) has enticed substantial care because polycarbonate is transparent, amorphous, completely re-cyclable, prepared from normal resources, and the most broadly utilized engineering polymer. It can resist all kinds of adverse and extreme ecological circumstances. Also, it's useful in reducing the carbon footprint. Additionally, it depicts virtuous thermal as well as mechanical properties [4-8]. Furthermore, amorphous materials have a lot of valuable potential uses related to their optical and electrical properties. Numerous electronic devices are made up of Polycarbonates, such as vessels for food-storage owing to their heat resistance and toughness, reusable bottles of water, devices of safety, safety devices of sports, parts of automobiles, DVDs, and CDs [9, 10]. Polystyrene (PS), a multipurpose thermoplastic polymer, is a commercial polymer broadly utilized in different manufacturing areas and for biomedical and packaging uses. When combined with different colorants, other plastics, or additives, polystyrene (PS) is utilized for making toys, instruments, automobile parts, electronic parts, and so on [11, 12].

Within the big nanotechnology area, joining the inorganic filler and the matrix characteristics of polymer gives a fresh economic method for obtaining tailored materials having a high performance when they can give the essential steadiness as well as easy process-ability with remarkable optical characteristics. An essential inorganic bioactive such as nHAP particles have been purposely compounded with hydrogels to offer necessary biological and mechanical properties [5]. Hydroxyapatite, HAP, or calcium phosphate ($Ca10(PO4)6(OH)2$, has been regularly employed as scaffold or implanting materials in biomedical applications due to its unique biological action and physicochemical properties [6].

Furthermore, nHAp has a superior specific surface area and excellent mechanical and biological properties [7]. Here, the purpose behind the incorporation of HAp into the PC/PS matrix is to reduce the glass transition temperature (Tg) to the crystallinity degree and thus increase the amorphous phase of the PC/PS polymer matrix.

Thin films of polystyrene and polystyrene-nHAp nanocomposites were made via spin coating and exposed to ultraviolet irradiation. The optical band-gap values decreased within the range from 4.54 eV in neat PS to 4.45

eV in PS-nHA p nanocomposites in the PS-nHAp nanocomposites before the irradiation [13]. Ruchuan Liu et al. [14] studied the new development of the hybrid photovoltaic systems of inorganic semiconductors and organic conducting polymers.

The optical absorption coefficient's measurement, especially close to the essential edge of absorption, provides a standard technique for investigating optically created electronic transitions. Also, this gives certain concepts on the band structure and the energy gap in the crystalline as well as non-crystalline materials [15-16]. The investigation explained in the present research is connected to the optical and structural properties of the PC/PS-nHAP blend nanocomposites. The current study investigates the influence of nano-sized hydroxyapatite particles on the chemical, morphological, optical, and structural properties of 10% PC/PS blend nanocomposites.

Shalini Agarwal et al. [17] prepared polycarbonate/polystyrene blend nanocomposites reinforced with titanium dioxide and studied the structural properties of the composite blends. They found broad peaks related to the composite blend due to the well-known amorphous nature of PC/PS. XRD diffractograms of the nanocomposites show the humps of PC/PS together with the peaks of the TiO2 fillers. This confirms that the filler maintained its nanostructure in the composites.

Dana A. Tahir [18] prepared polymer composite PS-PC thin films and studied the optical properties of the samples. They found that the films exhibited low reflection and high transmittance, and the reflection values decreased with increasing frequency for all samples. With an increase in wavelength, both the refractive indices and extinction coefficient decrease. The optical band gap values for the PC/PS composite reduced from 3.9 eV to 3.3 eV.

2. MATERIALS AND METHODS

The coefficient of the optical absorption (a) can be computed from the spectra of optical absorption employing this equation (19]:

$$\text{Log } (I^{\circ}/I) = 2.303\ A = \alpha\ t \quad (1)$$

Where:
I^{o}: Incident beam intensity
I: Transmitted beam Intensity
A: The optical absorbance
t: Thickness of film

Transmission coefficient (T) can be computed by the following equation:

$$T = 10^{-A} \quad (2)$$

Whereas the reflection values from the coefficient of absorption as well as the transmission were obtained using this equation:

$$R = 1- (A + T) \quad (3)$$

Transitions absorption edge can be determined according to the model suggested via Taucas:

$$ahv = C_o\ (hv-E_g^{opt})^n = g \quad (4)$$

Where the energy, which isn't a dependent constant, is connected with the valence as well as the conduction bands' properties, hv is the energy of photons, and Eg is the material optical energy band-gap. The n value for the permitted direct transmission is taken as (0.5). Variation of the (ahv)2 versus the (hv) gives a virtuous straight line fit to the absorption edge, and the extrapolation (hv) of $(ahv)^2 = 0$ gives the E_g^{opt}.

All the materials that were used in this work are of reagent grade and high purity. Hydroxyapatite with a purity of 97% and a size of 25 nm was purchased from Germany, Polycarbonate was bought from Japan, and the polystyrene was purchased from America dichloro methane (DCM) from Sigma-Aldrich Company.

PC and PS were used as precursors and were taken in (100/0, 10%, and 0/100) weight ratio and melted in the solvent (DCM). The nHAp powder was added with ratios of (0.8, 1.6, 3.2, 6.4, and 10 wt%) and mixed until homogeneous solutions were produced. The resulting solution was cast as well as dehydrated onto the glass Petri dish. The self-sustainable film was peeled off from this.

3. RESULTS AND DISCUSSION

3.1. Mechanical properties

The mechanical properties of polymer systems rely on factors such as stiffness, inter-molecular force chains, and molecular symmetry [20]. Figure 1 shows the stress-strain curves of (nHAP/10%PC/PS) composite films with various weight ratios (0.8, 1.6, 3.2, 6.4, and 10 wt. percent) of (n HAP). The even distribution of the inorganic fillers in the (10%PC/PS) matrix of the polymer was responsible for the improvement of the mechanical properties up to (1.6 wt.%) for the nHAP/10%PC/PS.

The polymers having a high crystallinity degree, rigid chains, or crosslinking possessed a high strength or limited elongation, causing a high modulus of elasticity, a high yield stress, a high stress at the peak value, and a low value of elongation.

The increase in strength is due to the increase in the interfacial adhesion between the matrix and the nanoparticles, which causes less sliding between the composite layers when stress is applied (21, 22].

Tensile strength is decreased due to particle agglomeration beyond the crucial content, as well as an increment in the non-uniformity [23, 24]. The lack of interfacial adhesion between the fillers and the polymer was responsible for the reduction in tensile strength [22].

Nevertheless, the modulus of elasticity, as well as the tensile strength of the composite film, was considerably reduced with the increment in the content of nHAP till (1.6 wt.%)

due to the generation of a harsh agglomeration and the exposure of nanoparticles as flaws in the fibers, causing the reduced tensile strength with a fragile and brittle property. See Figure 2.

The best sample is (10%PC/PS+1.6 nHAP) in mechanical properties, so it has been chosen in the present work to conduct the other tests.

It is seen that the tensile properties have been hermetically decreased by the increase of hydroxyapatite concentration due to the agglomeration formation during the processing of composite above 1.6 wt% hydroxyapatite in PC/PS; the main reason behind this is hydroxyapatite content reduces hydrogen bonds formation and its effect is higher than crosslink bonds formation, which decreases the tensile strength and the elongation at break, these results agree with [25].

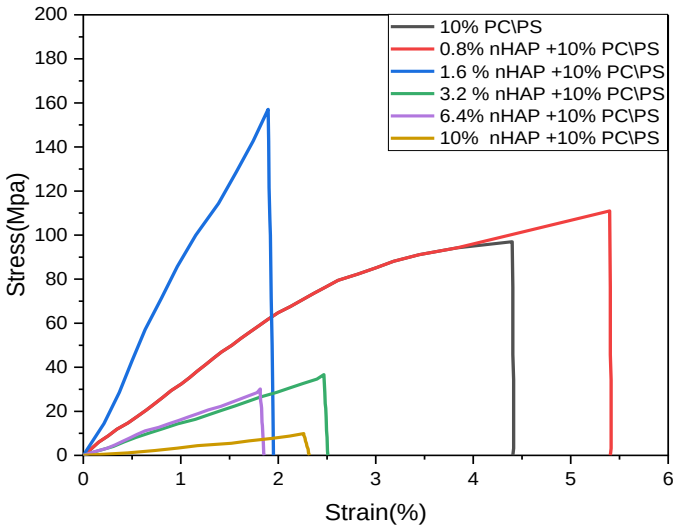

Figure 1 The stress-strain curve of (n HAP with 10%PC/PS) films

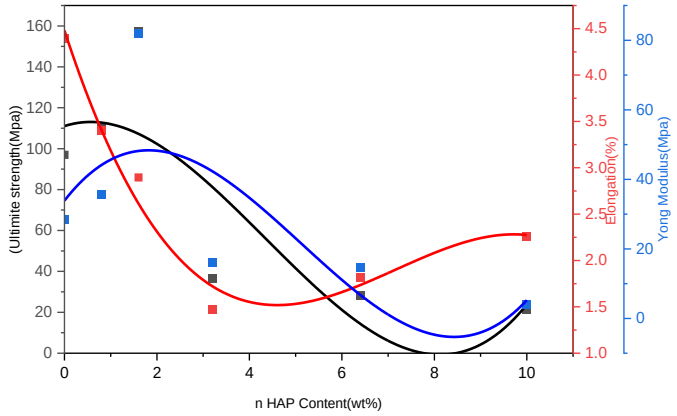

Figure 2 Ultimate tensile strength, Elongation, and Young's modulus of (10%PC/PS) films with different nHAP contents

3.2. X-ray diffraction (XRD)

XRD of the prepared nHAP nanoparticles, as well as the nHAP-PC/PS mixture nanocomposites, was registered employing Bruker D8 Advance with CuKα radiation (λ=1.54 Å), in the 2θ range (10°-80°). The X-ray diffractogram of the nHAP nanoparticles and a typical XRD pattern of 10%/PS/PC with its nHAP mixture nanocomposites are depicted in Figure 3.

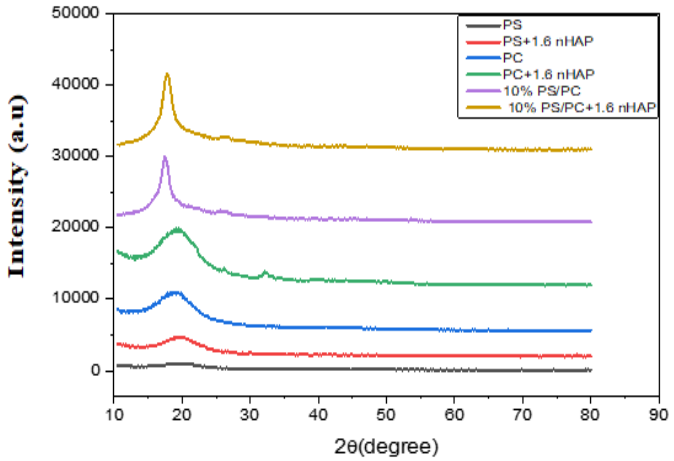

Figure 3 XRD patterns of the melt casting PC, PS, and PC/PS blends

All the XRD patterns are diffuse in shape, which is indicative of the amorphous nature of polymers. Pure PC reveals a single diffuse XRD peak centered at 2θ~18.2°, which is known to be due to the interference between the chains (Mitchell and Windle [26]; Windle [27]). Similarly, pure PS also indicates a broad peak centered at 2θ~19.3°. In the PC/PS blend, as the PC content increases, a significant shift in the characteristic XRD peak of PC (at 2θ~18.2) towards a higher two-theta side is observed. The inset to Figure 3 illustrates a variation of the peak position of the characteristic peak of PC with a variation in the content of PS in PC/PS blends. This again suggests an interaction between PC and PS phases in melt casting PC/PS blends [28].

The sharp crystalline reflections' appearance depicts the high nanoparticle purity as well as crystallinity. Their mean crystallite size was assessed, in accordance with the Scherrer formula [29], as (~19 mm). From the other side, the 10%PS/PC diffractogram exhibits wide reflections indicative of its amorphous feature. Such sharp peaks in the mixture nanocomposites diffractograms, collected with the nanoparticles features, verify that the nanoparticles' crystalline structure is affected by the structure of the mixture and turned it into a more crystalline structure in the mixture nanocomposite.

Hydroxyapatite peaks are located in the 2θ = 20°. As can be seen, low- and strong-intensity peaks appear when hydroxyapatite concentrations are low and high, respectively. Figure 3 shows pure PS and PC without hydroxyapatite, and it is shown that the intensity is very low, with broad peaks indicating the amorphous nature of the polymer. With the addition of hydroxyapatite with a concentration of 1.6 wt.%, the intensity increases, and the composite becomes crystalline, which leads to higher mechanical properties, as seen in the results; these results agree with [25].

3.3. Fourier Transform Infrared (FTIR)

A FTIR spectrum was used for the structural characterization of the mixture nanocomposites. FTIR spectroscopy is a powerful tool for identifying and investigating the different functional groups that exist in polymers. FTIR was achieved in the transmission mode employing Bruker Alpha-T spectrometer. And the spectra were registered in a wavenumber range of (500-4000 cm^{-1}). Table 1 shows the absorption band modes seen in the spectra of FTIR.

Figure 4 manifests the spectra of the FTIR of 10%PS/PC (wt/wt) with nHAP (0.8, 1.6, 3.2, 6.4, and 10 wt%) nanoparticles as a typical case. PC, PS, and nHAP absorption bands were seen in the IR spectrum.

In the case of hydroxyapatite, the absorption band at 568 and 606 cm^{-1} can be attributed to phosphate groups stretching vibrations. Also, the absorption band at 1422 cm^{-1} can indicate carbonate groups. Wide peaks at 1639 and 3570 cm^{-1} are related to the water that exists in the hydroxyapatite structure; these results agree with [25].

Table 1 Absorption band modes seen in the spectra of FTIR

S. No.	Mode	Wavenumber $(cm)^{-1}$
1	C=O stretching band	1773
2	Ring (C-C) vibrational mode	1507
3	O-C-O stretching vibrational mode	1013
5	Aliphatic C-H stretching	2849
6	Aromatic C=C stretching	1601, 1493
7	C-H deformation vibration band of benzene ring	758
8	Ring deformation vibration	700
9	Stretching vibration of hydroxyl(-OH)	3571.54
10	$(PO4)^{3-}$	1031.91
11	phosphate groups stretching	568-606
12	carbonate groups	1422

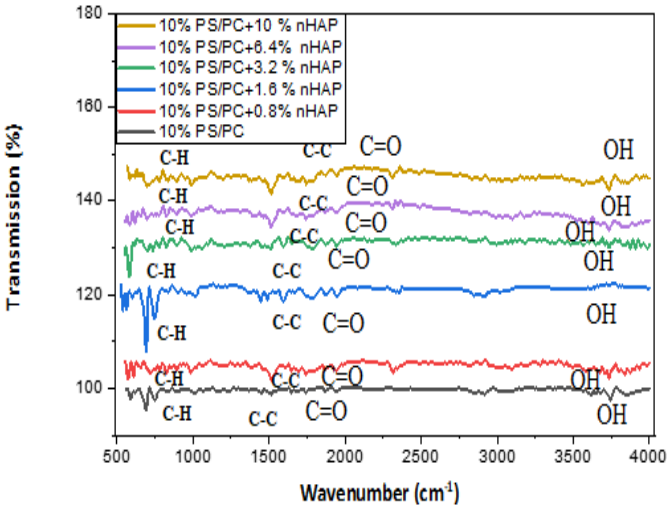

Figure 4 Spectra of the FTIR of 10PS/PC with its nHAP blend nanocomposites

3.4. Scanning Electron Microscopy (SEM)

SEM gives valuable info about the filler particle size and position upon the material surface. Zeiss EVO 18, an SEM device, was used to investigate the nanoparticle distribution in the matrix of the polymer mixture. Figure 5 evinces the images of SEM images (100%PC, 10%PS/PC, and PS100%) entrenched with (1.6 wt%nHAP) as typical cases. The nanoparticles of nHAP have a trend for agglomerating owing to their high surface energy. The arbitrary as well as the uniform homogeneous distributions of HAP were noticed in the polymer mixture nanocomposites.

It is shown that aggregation of the particles is not observed due to the low concentration of nanoparticles. As the hydroxyapatite concentration in the films increases, the aggregation of hydroxyapatite particles increases in the matrix, and their clusters are shown in Figure 5(c). They present SEM images of the surface of the nanocomposite films at two different regions. They show the surface using highly concentrated hydroxyapatite. The formation of cauliflower-like hydroxyapatite nanoparticles has been indicated on the surface of the starch matrix that dispersed uniformly in the matrix; these results agree with [25].

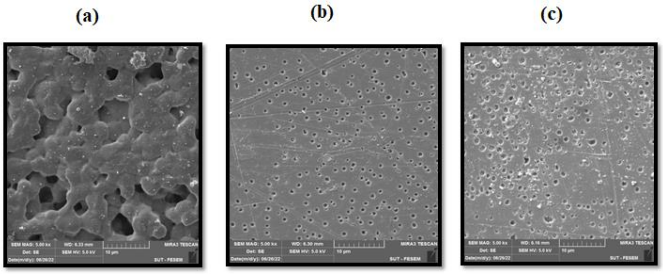

Figure 5 The images of SEM: (a) PC100%+1.6%nHAP, (b) 10%PS/PC+1.6 nHAP, and (c) PS100% +1.6% nHAP mixture nano-composites

3.5. UV-Vis Spectroscopy (UV VIS)

Perkin Elmer LAMBDA-750 UV/Vis/NIR spectrophotometer was used for recording the spectra of absorption in a (200-1200 nm) wavelength range. The mixture nanocomposites' absorption spectra below the test are portrayed in Figure 6. The redshift, i.e., higher absorption, was noted in the nHAP mixture nanocomposites in comparison with the neat matrix of the polymer.

The absorption rises as the content of nHAP rises owing to the incident light absorbance via the free charge carriers. Such spectra of absorption were utilized for calculating the band-gap employing the Tauc relationship (Eq. 4). The change of $(\alpha h\nu)2$ versus the $(h\nu)$ and the computation of band-gap in accordance with the Tauc relationship are demonstrated in Figure 7, as well as the band-gap values are listed in Table 2. A reducing tendency in the optical band-gap values was noted with the increment in the nHAP wt% in the polymer mixture samples below the test. The band-gap (4.22 eV) obtained for 10%PS/PC having a content of 1.6 nHAP is lesser than that for the neat PS, PC, and PS/PC mixture.

It is interpreted that the increase in transparency value is a result of light scattering in the interface between hydroxyapatite nanoparticles and the polymer matrix. Also, the crystalline structure of hydroxyapatite scatters the light and decreases the transparent film. Moreover, the high concentration of the nanoparticles improves the number of them in the polymer matrix and increases transparency value; these results agree with [25].

Table 2 Band-gap values for the PC/PS-nHAP mixture nanocomposites

Sample	Band-gap (eV)
PC Pure	4.39
PS Pure	4.41
10%PS/PC Pure	4.3
10%PS/PC+0.8%nHAP	4.29
10%PS/PC+1.6%nHAP	4.22
10%PS/PC+3.2%nHAP	4.21
10%PS/PC+6.4%nHAP	4.1
10%PS/PC+10%nHAP	3.8

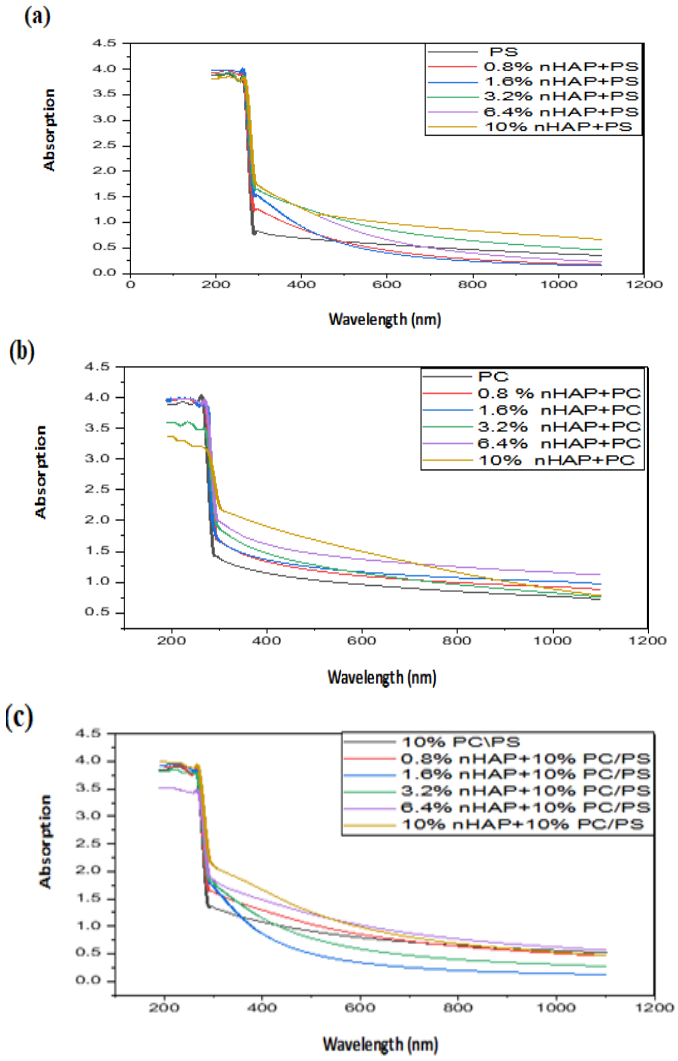

Figure 6 The absorption spectra for nHAP mixture nanocomposites of: (a) PS100%, (b) PC100%, and (c) 10%PS/PC

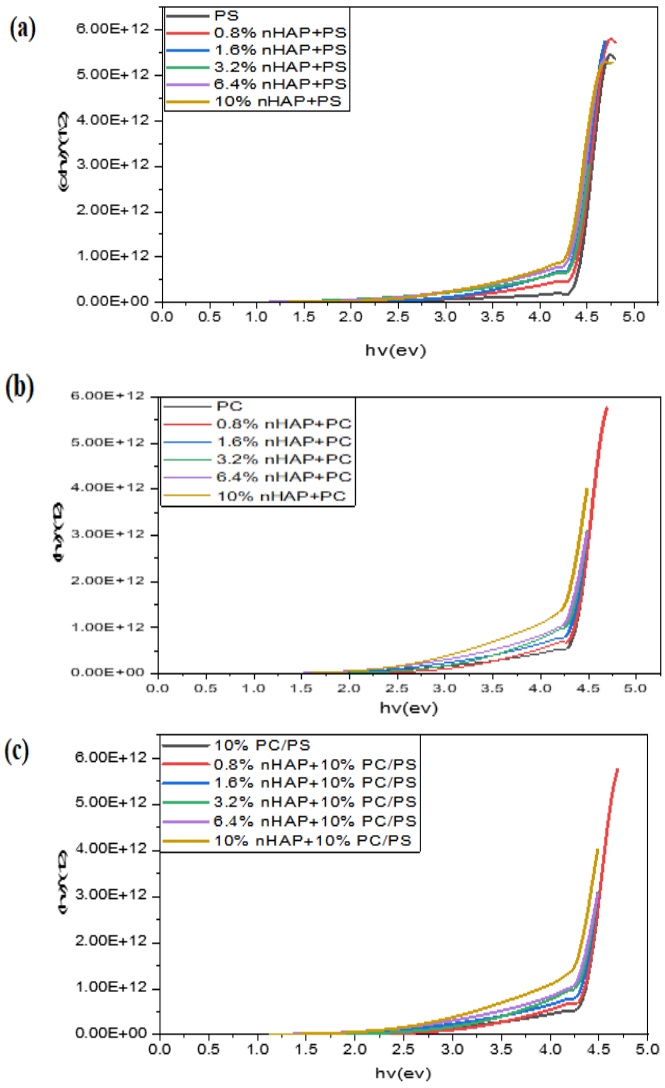

Figure 7 T The band-gap computation for nHAP mixture nanocomposites of (a) PS100%, (b) PC100%, and (c) 10%PS/PC

4. CONCLUSION

The results of the present investigation have led to the following conclusions: a group of nanocomposites of the PC/PS-nHAP blend was made via a solution casting technique. The mean crystallite size of the chemically prepared nanoparticles of nHAP was measured using the Scherrer formula and was (~19 mm). Results of the nanocomposites show that the nanoparticles stay in the nano-regime through the mixture nanocomposites preparing procedure. The FTIR spectra showed the existence of different functional groups in the mixture of nanocomposites, confirming the formation of polymer mixtures and nanocomposites. The SEM analysis provided information about the nHAP uniform dispersion in the polymer mixture nanocomposites. An increase in absorption peaks was observed by increasing the content of nHAP in the matrix of PC/PS. The optical band gap was reported to be reducing with the increase in the nHAP content in the nanocomposites blend system. The lowermost band-gap (4.22 eV) was obtained for 10%PS/PC with a content of 1.6% nHAP. Also, the PC/PS mixture nanocomposites with adapted nano hydroxyapatite are beneficial for food packaging uses.

ACKNOWLEDGMENTS

The authors would like to thank the Applied Science Department, University of Technology- Iraq, for the logistic support for this work.

REFERENCES

[1] A. Ariffin and M. S. B. Ahmad, "Journal of Polymer-Plastics Technology and Engineering," vol. 50, pp. 395-403, 2011.
[2] S. Agarwal, N. S. Saxena, R. Agrawal, and V. K. Saraswat, "AIP Conference Proceedings," vol. 1536, p. 777, 2013.
[3] S. Agarwal and V. K. Saraswat, "International Journal of Engineering Technology, Management and Applied Sciences," vol. 5, pp. 2349-4476, 2017.
[4] S. Agarwal, Y. K. Saraswat, and V. K. Saraswat, "Macromol. Symp.," vol. 357, pp. 70-73, 2015.
[5] S. Agarwal, Y. K. Saraswat, and V. K. Saraswat, "Journal of Open Physics," vol. 3, p. 63, 2016.
[6] S. Agarwal and V. K. Saraswat, "Optical Materials," vol. 42, pp. 335-339, 2015.
[7] B. N. Jang and C. A. Wilkie, "Thermochimica Acta," vol. 426, pp. 73-84, 2005.
[8] Y. Kitahara, S. Takahashi, M. Tsukagoshi, and T. Fujii, "Chemosphere," vol. 80, p. 1281, 2010.
[9] M. A. Corres, M. Zubitur, M. Cortazar, and A. Mugicaa, "Journal of Analytical and Applied Pyrolysis," vol. 92, pp. 407-416, 2011.
[10] V. K. Saraswat, V. Kishore, Deepika, K. Sharma, N. S. Saxena, and T. P. Sharma, "Chalcogenide Letters," vol. 4, p. 61, 2007.
[11] L. F. A. Pinto, B. E. Goi, C. C. Schmitt, and M. G. Neumann, "Journal of Research Updates in Polymer Science," vol. 2, p. 39, 2013.
[12] M. Pawde and S. S. Parab, "Pramana - Journal of Physics, Indian Academy of Sciences," vol. 70, p. 935, 2008.
[13] I. Y. Jeon and J. B. Baek, "Materials," vol. 3, p. 3654, 2010.
[14] D. Sun, N. Miyatake, and H. J. Sue, "Nanotechnology," vol. 18, p. 1, 2007.
[15] D. R. Paul and L. M. Robeson, "Journal of Polymer," vol. 49, pp. 3187-3204, 2008.
[16] L. L. Beecroft and C. K. Ober, "Chem. Mater.," vol. 9, p. 1302, 1997.
[17] S. Agarwal, Y. Saraswat, and V. Saraswat, "Polystyrene Blend Nanocomposites," *Macromolecular Symposia*, vol. 357, pp. 70-73, 2015.
[18] D. A. Tahir, "Optical properties of polymer composite PS-PC thin films," *Journal of Kirkuk University – Scientific Studies*, vol. 5, no. 2, 2010.
[19] J. Ballato and S. Foulger, "J. Opt. Soc. Am. B," vol. 20, no. 9, pp. 1838-1843, 2003.
[20] A. Devaraju, P. Sivasamy, and G. B. Loganathan, "Mechanical properties of polymer composites with ZnO nanoparticles," *Mater. Today Proc.*, vol. 22, pp. 531–534, 2020.
[21] T. Noguchi, M. Endo, K. Niihara, H. Jinnai, and A. Isogai, "Cellulose nanofiber/elastomer composites with high tensile strength, modulus, toughness, and thermal stability prepared by high-shear kneading," *Compos. Sci. Technol.*, vol. 188, p. 108005, 2020.
[22] D. P. and S. K. Narayanankutty, "Styrenated phenol modified nanosilica for improved thermo-oxidative and mechanical properties of natural rubber," *Polymer Testing*, vol. 82, 2020.
[23] M. A. Ashraf, W. Peng, Y. Zare, and K. Y. Rhee, "Effects of Size and Aggregation/Agglomeration of Nanoparticles on the Interfacial/Interphase Properties and Tensile Strength of Polymer Nanocomposites," *Nanoscale Res. Lett.*, vol. 13, no. 1, p. 214, 2018.
[24] W. D. Callister Jr. and D. G. Rethwisch, "Material Science and Engineering," 9th ed., John Wiley, 2014.
[25] Z. Hadi, N. Hekmat, and F. Soltanolkottabi, "Composites and Advanced Materials," *Composites and Advanced Materials*, vol. 1, no. 1, pp. 1-10, 2022.
[26] M. M. El-Desoky, I. M. Morada, M. H. Wasfya, and A. F. Mansourb, "Title of the Paper," *IOSR Journal of Applied Physics*, vol. 9, no. 5, pp. 33-40, 2017.
[27] M. T. Ramesan, "Title of the Paper," *Polymer-Plastics Technology and Engineering*, vol. 51, pp. 1223-1230, 2012.
[28] B. Jaleha, M. S. Madada, M. F. Tabrizib, S. Habibia, R. Golbedaghic, and M. R. Keymaneshd, "Title of the Paper," *J. Iran. Chem. Soc.*, vol. 8, pp. 161-170, 2011.
[29] R. Liu, "Title of the Paper," *Materials*, vol. 7, pp. 2747-2765, 2014.